NJC

PAPER

View Article Online
View Journal

Cite this: DOI: 10.1039/c6nj03174a

Towards a global greener process: from solvent-less synthesis of molybdenum(VI) ONO Schiff base complexes to catalyzed olefin epoxidation under organic-solvent-free conditions†

Marina Cindrić,*[a] Gordana Pavlović,[b] Robert Katava[abcd] and Dominique Agustin*[cd]

Received (in Victoria, Australia) 10th October 2016, Accepted 6th December 2016

DOI: 10.1039/c6nj03174a

www.rsc.org/njc

Nine Schiff base ligands derived from *o*-hydroxyaldehydes (2-hydroxybenzaldehyde, 2-hydroxy-3-methoxybenzaldehyde, 2-hydroxy- 1-naphthaldehyde) and nine corresponding dioxomolybdenum(VI) complexes, *cis*-$[MoO_2L(CH_3OH)]$ or *cis*-$[MoO_2L(CH_3OH)]\cdot CH_3OH$ and dinuclear $[MoO_2L]_2$, have been prepared using the conventional solution-based method as well as mechanochemically, by liquid assisted grinding (LAG). All products have been characterised by means of IR spectroscopy, thermal analyses and also by powder and five molybdenum complexes by single crystal X-ray diffraction. The crystal structure analysis of mononuclear complexes reveal distorted octahedral Mo(VI) coordination by ONO donor atoms from a dianionic tridentate Schiff base ligand, two oxido oxygen atoms from the MoO_2^{2+} moiety and an oxygen atom from the MeOH molecule *trans* to the oxido oxygen atom. Due to the *trans* effect of the oxido oxygen atom, Mo–O(MeOH) is the longest bond distance within the Mo coordination sphere and it expected to be the point of maximum reactivity of the complexes. All complexes have been studied as pre(catalysts) for the epoxidation of *cis*-cyclooctene, cyclohexene and (*R*)-limonene using aqueous *tert*-butyl peroxide (TBHP) as the oxidant and in the absence of an organic solvent.

Introduction

The development of sustainable and environmentally friendly chemical processes integrating the twelve principles of *green chemistry* is a challenging quest for chemists.[1] The most important principles are diminishing the use of organic solvent, especially toxic, and increasing the use of catalysts in order to obtain selective and quick processes. The chemical transformations including (ep)oxidation are interesting since epoxides are key starting materials for a wide variety of products in organic chemistry. The most commonly used efficient non-catalyzed (ep)oxidation processes are not green. The new approaches and the development of synthetic procedures such as metal-catalyzed oxidation processes provide new insights into ecologically and economically more acceptable path in catalysis. The synthesis, structure and different properties of various high-valent metal complexes are described in a large number of articles and most of these complexes have shown to be very effective catalysts in epoxidation.[2] Molybdenum is one of the most used elements, especially within industrial processes.[3] The molybdenum(VI) $[MoO_2(acac)_2]$ complex used in many substitution reactions, was described as one of the best molecular (pre)catalysts for the homogeneous catalytic epoxidation of olefins with TBHP/decane in organic solvents.[4] Among the high number of molybdenum(VI) complexes tested in the epoxidation of alkenes, $[MoO_2L(ROH)]$ complexes of Schiff base ligands have proven to be active catalysts. Due to the ease of change of their steric and/or electronic properties by the appropriate choice of the corresponding aldehyde and amine components, Schiff bases have been used extensively.[5] Most of those catalyzed reactions are performed in an organic solvent.[6] Carrying out research in accordance with the principles of green chemistry is still a challenge for many laboratories.[7]

We have recently developed an organic-solvent free procedure for the epoxidation of alkenes, using molybdenum(VI) complexes as catalysts, coordinated with ONO or ONS ligands.[8] The catalysts are very often synthesized *via* classical methods, using a significant

---

[a] *University of Zagreb, Faculty of Science, Department of Chemistry, Horvatovac 102a, HR-10000 Zagreb, Croatia. E-mail: marina@chem.pmf.hr; Fax: +385 1 4606 341*

[b] *University of Zagreb, Faculty of Textile Technology, Department of Applied Chemistry, Prilaz Baruna Filipovića 28a, HR-10000 Zagreb, Croatia*

[c] *CNRS, LCC (Laboratoire de Chimie de Coordination), 205 route de Narbonne, BP 44099, F-31077 Toulouse Cedex 4, France. E-mail: dominique.agustin@iut-tlse3.fr; Fax: +335 63 351 910; Tel: +335 63 621 172*

[d] *Université de Toulouse, UPS, INPT, Institut Universitaire de Technologie Paul Sabatier, Département de Chimie, Av. Georges Pompidou, CS 20258, F-81104 Castres Cedex, France*

† Electronic supplementary information (ESI) available. CCDC 1508023–1508027 (compounds **2a**, **3**, **6**, **7** and **9**). For ESI and crystallographic data in CIF or other electronic format see DOI: 10.1039/c6nj03174a

amount of organic solvents. In order to increase the "green" contribution to a catalytic process, *i.e.* considering not only catalyzed transformation but also catalyst synthesis, one of the most promising additional approaches used is the preparation of a catalyst using a greener method.[9] The latest reports have shown that solvent-free synthesis and mechanochemistry have been developed as effective and rapid, ecological procedures for a wide range of different ligands and their corresponding metal complexes.[10]

Based on our previous investigations[11] on this topic we have been interested in exploring (a) a comparison between mechanochemical and solvent-based synthetic methods for preparing Schiff base ligands and their molybdenum(VI) complexes; (b) influence of Schiff base ligands substitutuents on the crystal structure and the catalytic properties of the corresponding metal complexes; and (c) the catalytic activity of the complexes in the epoxidation of olefins with aqueous TBHP as the oxidant under organic solvent free conditions.

Results and discussion

Ligands and complexes: synthesis and characterization

The Schiff base ligands, H_2L^{1-9} were obtained using a classical solution-based method (a) or by liquid-assisted mechanosynthesis by using an agate mortar or ball milling (b), *via* a typical condensation reaction between the appropriate substituted aldehyde and 2-aminophenol or its 4- and 5-methyl derivatives (Scheme 1 and Table 1). Due to the different colours and in some cases different aggregation states of the reactants, the progress of the liquid-assisted mechanosynthesis can be readily monitored using a camera.

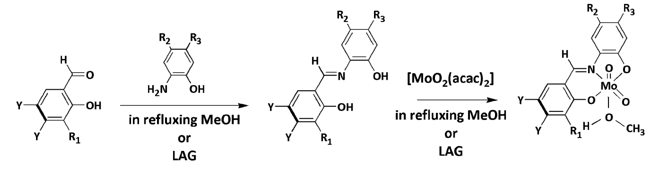

Scheme 1 Two synthetic paths of molybdenum(VI) complexes and ligands.

Table 1 Schiff base ligands and related complexes

H_2L^{1-9}	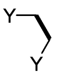	R_1	R_2	R_3	Complexes, **1–9**
H_2L^1	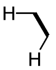	H	H	H	$[MoO_2L^1(CH_3OH)]$ **1**
H_2L^2		H	Me	H	$[MoO_2L^2(CH_3OH)]^a$ **2**
H_2L^3		H	H	Me	$[MoO_2L^3(CH_3OH)]\cdot CH_3OH$ **3**
H_2L^4		OMe	H	H	$[MoO_2L^4CH_3OH]$ **4**
H_2L^5		OMe	Me	H	$[MoO_2L^5(CH_3OH)]$ **5**
H_2L^6		OMe	H	Me	$[MoO_2L^6(CH_3OH)]\cdot CH_3OH$ **6**
H_2L^7	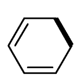	H	H	H	$[MoO_2L^7(CH_3OH)]$ **7**
H_2L^8		H	Me	H	$[MoO_2L^8]_2$ **8**
H_2L^9		H	H	Me	$[MoO_2L^9(CH_3OH)]\cdot CH_3OH$ **9**

[a] $[MoO_2L^2(CH_3OH)]\cdot CH_3OH$ **2a** unstable solvatomorph of **2** prepared and characterized.

The required time for grinding in the agate mortar was determined empirically when the colour of the reaction mixture stopped changing. All products were obtained as solid powders. The IR spectra, analytical data and results of PXRD experiments for all ligands obtained using both methods matched well (Table S1 and Fig. S1–S6, ESI†). The obtained results were in agreement with the literature data[12] for solvent free syntheses of Schiff base ligands derived from 2-amino-5-methylphenol and 2-hydroxybenzaldehyde (H_2L^3) and 3-methoxy-2-hydroxybenzaldehyde (H_2L^6) respectivelly, or from 2-amino-4-methylphenol and 2-hydroxybenzaldehyde (H_2L^2).

Dioxomolybdenum(VI) complexes, **1–9** (Table 1) have also been obtained using both methods. In the synthesis of all complexes, a very suitable, easily accessible precursor $[MoO_2(acac)_2]$ was used. Herein, we report for the first time liquid-assisted mechanosynthesis of nine dioxomolybdenum complexes containing Schiff base derivatives of 2-hydroxybenzaldehyde (H_2L^{1-3}), 3-methoxo-2-hydroxybenzaldehyde (H_2L^{4-6}) and 2-hydroxy-1-naphthaldehyde (H_2L^{7-9}) with 2-aminophenol and its 4-methyl- and 5-methyl derivatives (Scheme 1).

Five complexes, mononuclear $[MoO_2L^1(CH_3OH)]$ (**1**), $[MoO_2L^2(CH_3OH)]$ (**2**) $[MoO_2L^2(CH_3OH)]\cdot CH_3OH$ (**2a**), $[MoO_2L^5(CH_3OH)]$ (**5**) and dinuclear $[MoO_2L^8]_2$ (**8**), were prepared using the classical solution-based method reported in the literature.[11] Complex **2a** of the general formula $[MoO_2L^2(CH_3OH)]\cdot CH_3OH$ is unstable; a red solvatomorph of the orange complex **2** has been previously reported by us.[11] Similar synthetic conditions are used in the synthesis of five new complexes $[MoO_2L^3(CH_3OH)]\cdot CH_3OH$ (**3**), $[MoO_2L^4(CH_3OH)]$ (**4**), $[MoO_2L^6(CH_3OH)]\cdot CH_3OH$ (**6**), $[MoO_2L^7(CH_3OH)]$ (**7**) and $[MoO_2L^9(CH_3OH)]\cdot CH_3OH$ (**9**).

Applying the classical solution-based method and liquid-assisted mechanosynthesis, the replacement of the acetylacetonate ligands with a tridentate ligand L^{2-} produced mononuclear and/or dinuclear octahedrally coordinated molybdenum(VI) complexes. During the milling of the mixture of $[MoO_2(acac)_2]$ and H_2L^8 and formation of complexes **8** the colour of the reaction mixtures changed from orange to orange-green. Addition of a few drops of methanol changed the colour of the mixture back to orange. This behaviour is probably caused due to the important role of solvent molecules in the stability of the intermediate during the formation of these binuclear complexes. This behaviour is not observed during the preparation of any other complex (Fig. S7–S15, ESI†).

The $[MoO_2L^1(D)]$ complexes derived from 2-hydroxybenzaldehyde and 2-aminophenol (H_2L^1), coordinated with different solvent molecules (D = water, DMSO, alcohol, THF, imidazole, pyridine-*N*-oxide), have been reported in the literature so far.[13–15]

To examine the thermal stabilities of the prepared complexes, they are heated in an oxygen atmosphere from 25 °C to 600 °C. All complexes display very similar thermal behavior and small differences could be coupled with the observed structural differences. Thermal analysis data for complexes obtained using a solution based method, *cis*-$[MoO_2L^{1,2,4,5,7}(CH_3OH)]$ and $[MoO_2L^{2a,3,6,9}(CH_3OH)]\cdot CH_3OH$, reveal a well-defined endothermic step in the range from 38 to 232 °C, corresponding to the loss of only coordinated methanol molecules in **1** (64–158 °C), **2** (42–110 °C), **4** (60–123 °C), **5** (43–154 °C), and **7** (48–125 °C) or solvated and coordinated in **2a** (53–117 °C), **3** (38–169 °C), **6** (52–143 °C), and **9** (50–132 °C). The relatively labile binding of methanol molecules in the solid state is evident. The second step, in the temperature range of 200 to 580 °C is followed by the decomposition of [MoO_2L]. This stage includes highly exothermic oxidative reactions and the complete loss of organic matter, with MoO_3 being the final residue. Thermal analysis data for the [MoO_2L^8]$_2$ complex correspond to a one-step decomposition process in the range 266–514 °C. The thermal behavior of complexes prepared using the LAG method showed differences relative to the complexes obtained from the solution, certainly due to the fact that complexes prepared using the LAG method do not contain solvent of crystallization or some of them are polymers. The data for complexes obtained using the LAG method are given in Table S2 (ESI†) and compared with those obtained using the solution-based method.

The infrared spectra of all the prepared complexes (by both methods) exhibit bands characteristic of these types of complexes and all data are in accordance with the literature data.[13,14] The IR spectra of *cis*-[$MoO_2L^{1,2,5,7}(CH_3OH)$] and [$MoO_2L^{2a,3,6,9}(CH_3OH)$]·$CH_3OH$ complexes exhibit strong vibrations between 960 and 890 cm^{-1}. The appearance of two (or three) bands in this region is characteristic of *cis*-MoO_2 species. The presence of only a single stretch at about 930 cm^{-1} in the spectra of some complexes prepared using method (a) (*e.g.* [MoO_2L^8]$_2$) or (b) (*e.g.* complexes **4**, **7** and **8**) instead the usual doublet of MoO_2 suggests polymerisation *via* oxo bridging between molybdenum centres. The presence of stretching vibrations at about 870 and 750 cm^{-1} confirms the presence of oxo bridging, Mo–O···Mo. Several medium to weak bands in the region 550–650 cm^{-1} are assigned to $Mo–O_{(PhO)}$ stretching vibrations. The strong to medium bands in the region 1625–1160 and 1440–1300 cm^{-1} are assigned to C=N and phenolic C–O stretching vibrations, respectively (Table S3, ESI†).

Molecular and crystal structure of complexes 2a, 3, 6, 7 and 9

The aim of the work was to find out the possible correlation between the crystal structure and the catalytic activity of complexes. Complexes **2a**, **3**, **6** and **9** (general and crystallographic data are given in Table S4, ESI†) contain one methanol solvent molecule per complex molecule in the asymmetric unit, while complex **7** crystallizes without solvent of crystallization. The metal center is ligated by two terminal oxygen atoms and one tridentate dianionic Schiff base ligand coordinating *via* the phenolic oxygen atom, the imine N atom and the hydroxyl oxygen atom to the metal center (Fig. S16(a)–(e), ESI†). The sixth coordination site is occupied by the oxygen atom from the coordinated methanol molecule (Table S5, ESI†). The molybdenum oxido groups of the MoO_2^{2+} moiety show the expected mutual *cis* configuration and are located *trans* to the imine N atom and the coordinated MeOH molecule. The longest bond distance within the Mo coordination sphere is Mo–O(MeOH), due to the *trans* effect of the oxido oxygen atom, and it is expected to be the point of maximum reactivity of the complex. The axial octahedral angle around Mo(VI), which is constrained by the stereochemical rigidity of the ligand itself, exhibits the largest deviation from the ideal value approximately around 170° in all complexes (Table S6, ESI†). The deformation of the octahedral *cis* angle values around the metal center is determined by the ligand planarity, the bicyclic system of two chelate rings which are slightly folded along the axis of the molybdenum–imino bond and by the offset of the metal centre apart from the chelate planes towards the terminal oxygen atom. The latter increases misalignment of the planes defined by the chelate ring atoms from coplanarity with the planes of the peripheral aromatic systems (phenyl or naphthyl rings) (Table S5, ESI†). The Mo(VI) is shifted from the equatorial plane of the octahedron towards the terminal oxygen atom and the calculated dihedral angles exhibit that the largest deviation from coplanarity occurs in complexes **3**, **6** and **9** which contain solvent of crystallization or the $–OCH_3$ group (*vs.* $–CH_3$ group). These conformational discrepancies are caused by intermolecular interactions, formed by a methoxy group which is known to have formation capability as a proton acceptor. Namely, complex **6** is the only one containing both methanol solvent of crystallization and a methoxy group.In contrast, complex **7** does not contain methanol solvent of crystallization or a methoxy group and its chelate and aromatic ring systems are almost coplanar.

The crystal structures of complexes **2a**, **3**, **6**, **7** and **9** are dominated by two types of hydrogen bonds: O–H···O and C–H···O. The main supramolecular motif (Fig. 1) made by the methanol molecule of crystallization is the infinite chain shaped by the O–H···O types of hydrogen bonds with the coordinated methanol –OH group and the oxido oxygen atom (Fig. 1b, c and e) for complexes **2a**, **6** and **9**, respectively. In all three structures the crystallized MeOH molecule acts as a proton donor and acceptor simultaneously; with the oxido oxygen atom as the proton donor and with coordinated MeOH as the proton acceptor bridging complex molecules in the crystal.

These 1D infinite chains are usually transversally supported by rings formed *via* C–H···O types of hydrogen bonds and consequently infinite ribbons of alternating condensed rings are formed. The main supramolecular pattern found in **3** and **7** is a centrosymmetric dimer formed by two molecules of solvent CH_3OH, which are joined by the O–H···O intermolecular hydrogen bond and further with two complex molecules *via* the phenolate O4 oxygen atom (Fig. 1a). Since complex **7** does not contain solvent molecule of crystallization, the main supramolecular synthon formed *via* the O–H···O hydrogen bond is a centrosymmetric dimer between the –OH group of coordinated methanol and the O3 donor atom of the five-membered chelate ring of another complex molecule (Fig. 1d). Detailed descriptions of these supramolecular architectures are given in the ESI† (Fig. S21 and Table S7). The preliminary data of the molecular and crystal structure of the [$MoO_2L_4(CH_3OH)$] complex were accomplished using the PXRD method (Table S4, ESI†).

Catalytic activity of molybdenum complexes

The catalytic activity of all molybdenum complexes, prepared using the solution based method, was evaluated for the epoxidation of three substrates: *cis*-cyclooctene, cyclohexene and (*R*)-limonene. The influence of the ligand substitution was the

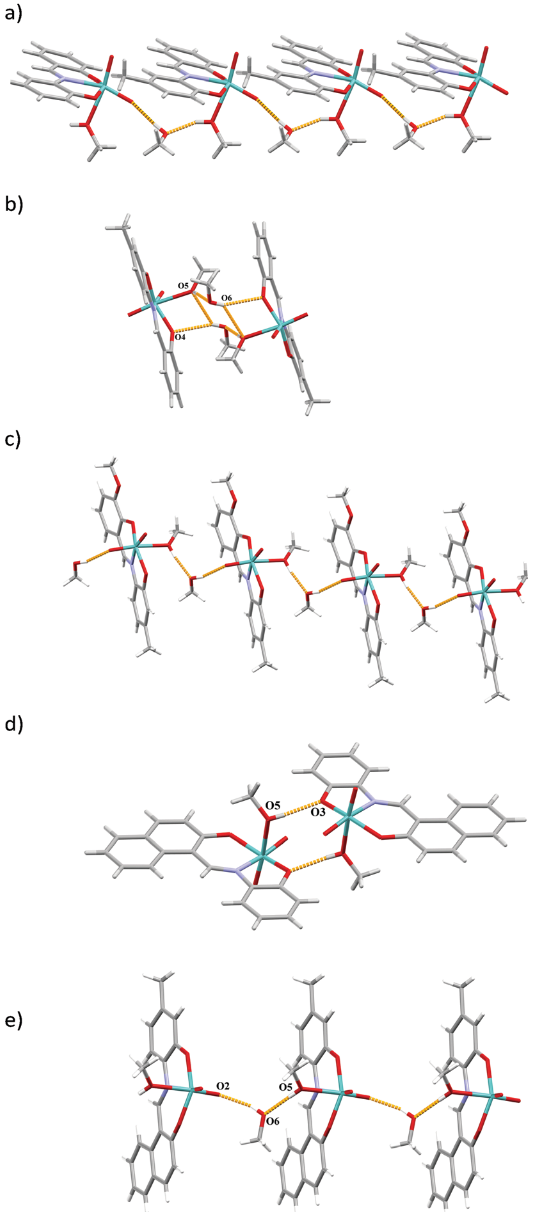

Fig. 1 Main supramolecular interactions shaped by the O–H···O types of hydrogen bonds with the coordinated methanol oxygen atom. (a) Infinite 1D chain formation along the *a* axis in **2a** *via* O1M–H1OM···O1A and O5A–H5O···O1M intermolecular hydrogen bonds. The methanol solvent molecule acts as a proton donor in hydrogen bond formation with the terminal oxido O1A atom and as a proton acceptor in hydrogen bond formation with a coordinated methanol molecule. (b) Formation of a supramolecular 8-membered hydrogen bonded ring *via* the O–H···O type of hydrogen bond in **3**. Further supramolecular linking between the complex and the solvent molecule by the O–H···O type of hydrogen bond. (c) Linking of the complex and solvent molecules in **6** into one-dimensional infinite chains spreading along the *b* axis *via* O7–H7···O2 and O5–H5···O7 intermolecular hydrogen bonds. (d) Formation of the centrosymmetric dimers *via* the O–H···O hydrogen bond between –the OH group of coordinated methanol and the O3 donor atom of the five-membered chelate ring of another complex molecule in **7**. (e) Infinite one-dimensional chains formation spreading along the *a* axis in **9** by solvent molecules of crystallization which act as a proton donor and aa proton acceptor *via* O5–H5···O6 (proton acceptor) and O6–H6···O2 (proton donor) intermolecular hydrogen bonds.

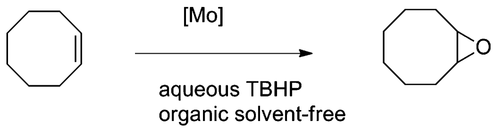

Scheme 2 Epoxidation of *cis*-cyclooctene catalysed by molybdenum complexes.

studied parameter. The prominence in these investigations was given to low Mo/alkene ratio (0.5%), all alkenes were (ep)oxidized by aqueous TBHP in the absence of organic solvent.

The complexes are moderately soluble in substrates and insoluble in water at room temperature, but dissolve in the organic phase after the addition of aqueous TBHP at 80 °C. The coloured organic phase suggests that, as previously observed with similar complexes, the catalyst is mostly confined in the organic phase. Catalysts containing a 3-methoxy substituent (**4–6**) showed best solubility and were dissolved within 10 min after the addition of TBHP. Catalyst **8** (binuclear complex) remained poorly dissolved in reactions with all three substrates, even after 4 h. As was previously described, coordinated methanol is released during catalysis. Catalysts **7** and **9** started to precipitate as the reaction advanced, certainly due to the release of coordinating methanol and formation of dimers.

Epoxidation reactions of cyclooctene, cyclohexene and limonene

Cyclooctene. Cyclooctene (CO) is considered in the literature as a model olefin for the epoxidation (Scheme 2). This substrate is a good indicator of epoxidation since few by-products are observed and the corresponding epoxide (COE) is sufficiently stable in the presence of water, as previously shown. A blank reaction without the catalyst showed very low conversion after 4 hours, exhibiting the activity of the complexes. Catalyzed epoxidation of *cis*-cyclooctene with all complexes led to conversion of CO between 68 and 86% with selectivity towards COE between 90 and 97%. A small portion of organic compounds are observed in the water phase since the mass balance in the organic phase (substrate + epoxide) is between 91 and 98%.

The comparisons can be made starting from the simple 2-hydroxybenzaldehydato backbone (L^1). Introduction of methyl in the R^2 or R^3 position did not change the catalytic results dramatically, with a slightly better conversion with complex **3** (R^3 = Me) and a better activity. When R^2 = Me (complex **2**), the compound seemed to be less active with a lower TOF.

Introduction of the methoxy group or the naphthyl group on the ligand backbone was noticeable in the catalytic results. For both changes, the conversion was higher than their corresponding methylated complexes on SAP backbones.

The most efficient catalyst was the complex possessing a naphthyl backbone substituted by one methyl in the *X*-position with 86% of CO conversion and 97% selectivity towards COE (and the highest TOF of 200) (Table 2).

During the catalytic process, complexes **4–6** (derived from 3-methoxy-2-hydroxybenzaldehyde) were soluble while complexes **7–9** (derived from 2-hydroxy-1-naphthaldehyde) were poorly soluble.

Table 2 The epoxidation of cyclooctene with TBHP using Mo(VI) complexes

Mo cat.[a]	CO conversion[b] (%)	Selectivity towards COE (%)	TOF[c]/h^{-1}	TON[d]
No cat.	2	23		
1	68	92	117	135
2	68	91	74	135
3	75	91	158	148
4	83	94	164	165
5	74	94	138	147
6	80	92	153	157
7	80	93	105	160
8	72	90	51	142
9	86	97	200	170

[a] Reaction conditions: time, 4 h; temperature, 80 °C; [Mo]/CO/TBHP molar ratio: 0.5/100/200. [b] Calculated after 4 h. [c] *n*(CO transformed)/*n*(catalyst)/time at 30 min. [d] *n*(CO transformed)/*n*(catalyst) at 4 h.

Table 3 The epoxidation of cyclohexene with TBHP using Mo(VI) complexes

	Conversion[b] (%)	Selectivity after 4 h (%)			
Mo cat.[a]	CH	CHO	CHD	TOF[c]/h^{-1}	TON[d]
No cat.	15	<1	23		
1	70	20	31	77	140
2	54	26	33	43	108
3	58	32	39	59	115
4	62	20	35	56	124
5	57	28	30	50	107
6	55	29	35	64	110
7	56	19	39	53	110
8	37	5	71	17	74
9	54	20	41	55	112

[a] Reaction conditions: time, 4 h; temperature, 80 °C; [Mo]/CH/TBHP molar ratio: 0.5/100/200. [b] Calculated after 4 h. [c] *n*(CH transformed)/*n*(catalyst)/time at 30 min. [d] *n*(CH transformed)/*n*(catalyst) at 4 h.

The low solubility does not seem to be a problem for the catalysis. It is probable that those complexes are slightly soluble and it is enough to be extremely active.

In accordance with the literature data[15] it has been observed that Lewis acidity of the catalyst helps in the ring opening process for small rings. The use of ligands with a methyl group in the R^2 position make the dioxomolybdenum(VI) complex (**2**, **5** and **8**) a weaker Lewis acid and showed worse results.

Cyclohexene. Cyclohexene (CH) showed to be an interesting model substrate for epoxidation tests under solvent free conditions. Indeed, without using a catalyst and using TBHP in water only, CH was poorly converted (7%) and the corresponding expected epoxide (CHO) was detected in very low quantity (Scheme 3). When the catalyst was added, conversions were observed and the presence of epoxide (CHO) and subsequent ring opening in the presence of water (*i.e.* the cyclohexanediol, CHD) could be observed in the organic phase. We have shown recently that a part of the diol is transferred in the aqueous phase (water being present because of the nature of the oxidant, *i.e.* TBHP in water). A GC analysis of the water phase showed that only diol was present, justifying this assumption. The control of the mass balance at the end of the reaction as for cyclooctene showed that between 60 and 80% of compounds (CH + CHO + CHD) are maintained in the organic phase (Table 3). All reactions in the presence of complexes exhibited higher conversion of cyclohexene, indicating their catalytic role.

The conversion values were between 54 and 70% (and 37% for complex **5**), depending on the nature the catalyst. As observed previously with similar complexes, the selectivity towards epoxide (CHO) lay between 19 and 32% (5% for the dimeric complex **8**), depending on the nature of the catalyst. Since CHD is soluble in water, the diol, consecutive to the CHO ring opening can be observed in all cases. The mass balance in the organic phase indicates that cyclohexanediol (CHD) is transferred into the water phase. [$MoO_2(L^1)(MeOH)$] was the best catalyst in terms of CH conversion. The trend showed that the presence of the naphthyl backbone gave slightly worse results but the influence of methyl and/or methoxy substitution was not very significant.

Limonene. Limonene (Lim) is an interesting substrate to study. Indeed, the intrinsic geometry around the double bond and the presence of isopropenyl can have an influence on the epoxidation, giving *cis* and *trans* 1,2-limonene epoxide (*cis*- and *trans*-LimO) (Scheme 4). The subsequent epoxide ring opening with water leads mainly to the *trans*-diaxial limonene-1,2-diol (LimD). This diol is also water-soluble. The analysis of the content of the organic phase was performed and the results are given in Table 4.

The analyses of all experiments at the end of the reaction show that epoxidation of (*R*)-limonene yielded *cis* and *trans*-LimO, and LimD for all complexes. The calculated mass balance in the organic phase at the end of the reaction showed that around 80% of the compounds (Lim + LimO (*cis* + *trans*) + LimD) are present in the organic phase. It has been shown in several articles that limonene diol (LimD) can be obtained

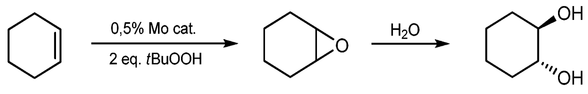

Scheme 3 Epoxidation of cyclohexene catalysed by molybdenum complexes using TBHP in water.

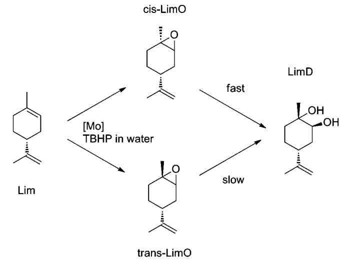

Scheme 4 Epoxidation of limonene catalysed by molybdenum complexes using TBHP in water.

Table 4 The epoxidation of limonene with TBHP using Mo(VI) complexes

Mo cat.[a]	Lim conversion[b] (%)	Selectivity (%) *cis*-LimO	*trans*-LimO	LimD	Max TOF[c] (h^{-1})	TON[d]
No	8	17		nd		
1	67	9	31	28	45	134
2	49	28	35	14	41	98
3	63	14	33	25	79	126
4	62	8	31	30	76	124
5	59	19	34	22	64	116
6	66	8	31	30	84	132
7	52	6	29	30	39	103
9	55	8	32	29	55	108

[a] Reaction conditions: time, 4 h; temperature, 80 °C; [Mo]/Lim/TBHP molar ratio: 0.5/100/200. [b] Calculated after 4 h. [c] *n*(Lim transformed)/*n*(cat.)/time at 30 min. [d] *n*(Lim transformed)/*n*(cat.) at 4 h.

mainly from *cis*-epoxide (LimO) in the presence of a molybdenum catalyst, or under acidic conditions. At the first few hours of the reaction the proportion of *cis* and *trans* is close, not showing selectivity between both stereoisomers. This phenomenon was also observed in our case with all the catalyst by a kinetic experiment. The plateau of 50% of each isomer was not reached showing that both epoxides are sensitive to water and are opened. However, the quantity of *cis*-LimO decreases very fast in contrast to *trans*-LimO, while the quantity of *trans*-diol increases at the same time.

Conclusions

LAG method can be used for the synthesis of molybdenum Schiff base complexes

A comparison between liquid-assisted grinding and solvent-based synthetic methods for preparing Schiff base ligands and their molybdenum(VI) complexes was explored. The complexes prepared using the LAG method showed differences in the properties and structures relative to the complexes obtained from the solution, certainly due to the fact that complexes prepared using the LAG method do not contain methanol solvent of crystallization.

Influence of substituents and solvent molecules on Schiff base ligands on the crystal structure of complexes

Conformational discrepancies caused by intermolecular interactions are observed only in the complexes which contain solvent of crystallization or the –OCH$_3$ group (*vs.* –CH$_3$ group) on the Schiff base backbone. These hydrogen bonds are formed between the methoxy group, which is known to have formation capability as a proton acceptor, and the solvent molecule.

Electronic influence of substituents on the Schiff base backbone alters Lewis acidity of the catalyst, which is crucial for its activity

(a) The molybdenum(VI) complex coordinated with Schiff's base derived from 2-hydroxybenzaldehyde and 2-aminophenol is the best catalyst in terms of cyclohexene conversion; (b) the presence of a naphthyl and methyl and/or methoxy group on the ligand backbone does not affect the catalytic results. Introduction of the methoxy and naphthyl groups on the ligand backbone is noticeable on the conversion of cyclooctene to the corresponding epoxide; and (c) the epoxidation of (*R*)-limonene yield *cis* and *trans* 1,2-limonene epoxide and *trans* diaxial limonene-1,2-diol for all complexes, present mostly in the organic phase.

Experimental

Materials and methods

Ligands H$_2$L$^{1-9}$ were prepared by Schiff's base condensation and by neat grinding according to the procedures described in the literature.[11b,12] The molybdenum precursor [MoO$_2$(acac)$_2$] was prepared according to the literature procedure.[16] Methanol was dried using magnesium turnings and iodine and then distilled. For the catalytic investigations *cis*-cyclooctene (98% Aldrich), cyclooctene oxide (Aldrich), limonene (Aldrich), limonene oxide (Aldrich), cyclohexene (Aldrich) cyclohexene oxide (Aldrich) TBHP (70% in water, Aldrich), H$_2$O$_2$ (35% in water, Aldrich) and diethyl ether (ACROS) were commercially available and used as received.

Catalytic reactions were followed by gas chromatography on an Agilent 6890A chromatograph equipped with an FID detector, a HP5-MS capillary column (30 m × 0.25 mm × 0.25 μm) and automatic sampling, or on a Fisons GC 8000 chromatograph equipped with an FID detector and with a SPB-5 capillary column (30 m × 0.32 mm × 0.25 μm). The GC parameters were quantified with authentic samples of the reactants and the products. The conversion of olefins and the formation of the corresponding oxides or diols were calculated from calibration curves (r^2 = 0.999) relatively to an internal standard.

Crystallography

Selected crystallographic and refinement data for structures corresponding to compounds **2a**, **3**, **6**, **7** and **9** obtained by the single-crystal X-ray diffraction experiment are summarized in Table S4 (ESI†). Selected geometries including valence bonds and angles, hydrogen bond geometry and $\pi\cdots\pi$ interactions are given in Tables S5 and S6 (ESI†), respectively. Data collection was performed on an Oxford Xcalibur diffractometer equipped with a CCD detector under graphite-monochromated MoK$_\alpha$ radiation (λ = 0.71703 Å) at room temperature (296(2) K) by employing the ω-scan technique. Programs CrysAlis CCD and CrysAlis RED (Versions 1.171.33.55 and 1.171.34.4)[17] were employed for data collection, cell refinement and data reduction. The intensity data were corrected for Lorentz and polarization factors as well as for absorption effects using a multi-scanning method.

The structures (**2a**, **3**, **6**, **7** and **9**) were solved using direct methods and successive Difference Fourier maps and refined by weighted full-matrix least-squares based on F^2 by using all unique data. Programs SHELXL2014[18] and SHELXL2014[19] integrated in the WinGX (v. 1.80.05)[20] software system were used to solve and refine structures. All non-hydrogen atoms were refined with anisotropic displacement parameters. The hydrogen atoms, except those from the coordinated or solvent methanol molecules, were treated by a riding model as they were placed on the basis of the conformation of the preceding carbon or nitrogen atoms with assigned isotropic displacement parameters. The hydrogen atoms belonging to the oxygen methanol molecule was firstly found in the difference Fourier map at the final stages of the refinement procedure and then refined by SHELXL2014 DFIX instruction at the O–H distance of 0.82(2) Å with assigned isotropic displacement parameters being 1.2 times larger than the equivalent isotropic displacement parameters of the parent oxygen atom. The positional disorder of the complex molecule in **3** has been resolved and fixed at major (A) and minor (B) component abundance in the final ratio of 57 : 43.

Due to the lack of a satisfactory parameter-to-data ratio (not to be less than 10) the non-hydrogen atoms of both components A and B have been refined anisotropically by applying a SHELXL2014 RIGU restraint on each of the two parts as well as ISOR instruction for O3A, O3B, O4A, O4B, O5A and O5B atoms.

The molecular geometry calculations especially including H-bonding and non-covalent interactions were performed using programmes PLATON and PARST95 integrated in the WinGX software system.[21] Program ORTEP-3,[22] also part of the WinGX software system, was used for molecular visualization. Packing diagrams were generated using Mercury.

The powder X-ray diffraction data were collected using a Panalytical X'Change powder diffractometer in the Bragg-Brentano geometry using CuK$_\alpha$ radiation. The sample was contained on a Si sample holder. Patterns were collected in the range of 2θ = 5–50° with the step size of 0.03° and at 1.5 s per step. The data were collected and visualized using the X'Pert program Suite.[23]

General procedure for the synthesis of complexes 1–9

Synthesis of the mononuclear complexes $[MoO_2(L^{1,2,4,5\text{ or }7})(MeOH)]$, $[MoO_2(L^{2a,3,6\text{ or }9})(MeOH)]\cdot MeOH$ and the binuclear complex $[MoO_2(L^8)]_2$.

(a) General method: solution-based synthesis for complexes. A mixture of $[MoO_2(acac)_2]$ (0.61 mmol) and the appropriate ligand H_2L^{1-9} (0.61 mmol) was refluxed for 4 hours in dry methanol (30 mL). The solution was left at room temperature for three days and the obtained crystalline precipitate was filtered off, rinsed with cold methanol and dried in air. The same products were obtained if the reactions were performed *in situ* without previous isolation of Schiff base ligands.

(b) General method: liquid-assisted mechanosynthesis (LAG) of complexes. All complexes were synthesized by liquid-assisted grinding together with equimolar quantities of the appropriate Schiff base ligand (0.15 mmol) and $[MoO_2(acac)_2]$ (0.15 mmol) in the presence of 30 μL of methanol. Grinding was performed in a stainless steel jar of 10 mL volume. A Retsch MM200 grinder mill operating at 25 Hz frequency was used for the synthesis.

In continuation are given analytical data for six new complexes (**3**, **4**, **6**, **7**, **9**) obtained using both methods, solvatomorphic form **2a** obtained using method (a) and four complexes (**1**, **2**, **5** and **8**) known from the literature obtained using method (b).

1: method (a) complex **1** has been prepared using the solution-based method according to the literature data.[11]

Method (b) $[MoO_2(L^1)(MeOH)]$ yield (yellow powder): 52.8 mg (46.4%). C, 44.7; H, 3.2; N, 3.6; Mo, 25.6%. Calc. for $C_{14}H_{13}MoNO_5$ (M_r = 371.22): C, 45.3; H, 3.5; N, 3.8; Mo, 24.7%. IR(KBr, cm^{-1}): 1611$\nu_{(C{=}N)}$; 935 and 907$\nu_{(MoO_2)}$.

2:·method (a) $[MoO_2(L^2)(MeOH)]\cdot MeOH$: yield (unstable red crystals): 19.8 mg (31%). C, 45.9; H, 4.6; N, 3.3; Mo, 22.9%. Calc. for $C_{16}H_{19}MoNO_6$ (M_r = 417.26): C, 46.1; H, 4.6; N, 3.4; Mo, 23.0%. IR(KBr, cm^{-1}): 1605$\nu_{(C{=}N)}$; 933 and 912$\nu_{(MoO_2)}$.

Method (b) $[MoO_2(L^2)(MeOH)]$: yield (orange powder): 35.4 mg (60%). Found: C, 46.7; H, 3.8; N, 3.6; Mo, 24.8%. Calc. for $C_{15}H_{15}MoNO_5$ (M_r = 385.26): C, 46.8; H, 3.9; N, 3.6; Mo, 24.9%. IR(KBr, cm^{-1}): 1606$\nu_{(C{=}N)}$; 935 and 907$\nu_{(MoO_2)}$.

3: method (a) $[MoO_2(L^3)(MeOH)]\cdot MeOH$: yield (red crystals): 75 mg (27.4%). Found: C, 45.9; H, 4.6; N, 3.3; Mo, 22.8%. Calc. for $C_{16}H_{19}MoNO_6$ (M_r = 417.26): C, 46.0; H, 4.6; N, 3.4; Mo, 23.0%. IR (KBr, cm^{-1}): 1614 $\nu_{(C{=}N)}$; 946 and 911 $\nu_{(MoO_2)}$.

Method (b) $[MoO_2(L^3)(MeOH)]$: yield (red powder): 22 mg (29.9%). Found: C, 45.9; H, 3.8; N, 3.7; Mo, 22.96%. Calc. for $C_{15}H_{15}MoNO_5$ (M_r = 385.26): C, 46.7; H, 4.2; N, 3.6; Mo, 24.91%. IR (KBr, cm^{-1}): 1613 $\nu_{(C{=}N)}$; 934 and 896 $\nu_{(MoO_2)}$.

4: method (a) $[MoO_2(L^4)(MeOH)]$: yield (yellow crystals): 100 mg (40.6%). C, 50.3; H, 3.5; N, 3.2; Mo, 23.5%. Calc. for $C_{15}H_{15}MoNO_6$ (M_r = 401.2): C, 44.9; H, 3.8; N, 3.5; Mo, 23.7%. IR(KBr, cm^{-1}): 1609$\nu_{(C{=}N)}$; 949 and 926$\nu_{(MoO_2)}$.

Method (b) $[MoO_2(L^4)]_2$: yield (dark yellow powder): 38 mg (33.6%). C, 50.3; H, 3.5; N, 3.2; Mo, 23.0%. Calc. for $C_{28}H_{22}Mo_2N_2O_{10}$ (M_r = 738.4): C, 45.5; H, 3.0; N, 3.8; Mo, 26.0%. IR(KBr, cm^{-1}): 1625$\nu_{(C{=}N)}$; 816 and 750$\nu_{(Mo_2O_2)}$.

5: method (a) complex **5** has been prepared using the solution-based method according to the literature data.[11]

Method (b) $[MoO_2(L^5)(MeOH)]$: yield (orange powder): 44.6 mg (35.0%). C, 45.9; H, 4.3; N, 3.1; Mo, 21.4%. $C_{16}H_{17}MoNO_6$ (M_r = 415.25): C, 46.3; H, 4.1; N, 3.4; Mo, 23.1%. IR(KBr, cm^{-1}): 1617$\nu_{(C{=}N)}$; 931 and 899$\nu_{(MoO_2)}$.

6: method (a) $[MoO_2(L^6)(MeOH)]\cdot MeOH$: yield (orange-red crystals): 190 mg (69.3%). Found: C, 44.9; H, 4.6; N, 3.0; Mo, 21.7%. Calc. for $C_{17}H_{21}MoNO_7$ (M_r = 447.26): C, 45.7; H, 4.7; N, 3.2; Mo, 21.5%. IR(KBr, cm^{-1}): 1624$\nu_{(C{=}N)}$; 899 and 882$\nu_{(MoO_2)}$.

Method (b) $[MoO_2(L^6)(MeOH)]$: yield (orange-red powder): 56.4 mg (44.3%). Found: C, 45.9; H, 4.6; N, 3.3; Mo, 23.6%. Calc. for $C_{16}H_{17}MoNO_6$ (M_r = 415.25): C, 46.3; H, 4.1; N, 3.4; Mo, 23.1%. IR(KBr, cm^{-1}): 1614$\nu_{(C{=}N)}$; 935 and 902$\nu_{(MoO_2)}$.

7: method (a) $[MoO_2(L^7)(MeOH)]$: yield (red crystals): 40.31 mg (62.5%). C, 51.3; H, 3.6; N, 3.0; Mo, 22.6%. Calc. for $C_{18}H_{15}MoNO_5$ (M_r = 421.3): C, 51.4; H, 3.4; N, 3.3; Mo, 22.8%. IR(KBr, cm^{-1}): 1609$\nu_{(C{=}N)}$; 934 and 910$\nu_{(MoO_2)}$.

Method (b) $[MoO_2(L^7)]_2$: yield (red powder): 50.0 mg (77.6%). C, 52.0; H, 3.0; N, 3.2; Mo, 23.7%. Calc. for $C_{34}H_{22}Mo_2N_2O_8$ (M_r = 784.4): C, 52.5; H, 2.8; N, 3.6; Mo, 24.5%. IR(KBr, cm^{-1}): 1609$\nu_{(C{=}N)}$; 812 and 742$\nu_{(Mo_2O_2)}$.

8: method (a) complex **8** has been prepared using the solution-based method according to the literature data.[11]

Method (b) $[MoO_2(L^8)]_2$: yield: 48.8 mg (dark brown powder) (79.2%). C, 51.3; H, 4.5; N, 3.0; Mo, 22.9%. Calc. for $C_{36}H_{26}Mo_2N_2O_8$ (M_r = 806.48): C, 53.6; H, 3.2; N, 3.5; Mo, 23.8%. IR(KBr, cm^{-1}): $1619\nu_{(C{=}N)}$; $824_{(MoO_t)}$ and $742\nu_{(Mo_2O_2)}$.

9: method (a) $[MoO_2(L^9)(MeOH)]\cdot MeOH$: yield (orange crystals): 110 mg (38.6%). C, 51.3; H, 4.5; N, 3.0; Mo, 19.9%. Calc. for $C_{20}H_{19}MoNO_6$ (M_r = 465.32): C, 51.6; H, 4.1; N, 3.0; Mo, 20.5%. IR(KBr, cm^{-1}): $1631\nu_{(C{=}N)}$; 900 and $885\nu_{(MoO_2)}$.

Method (b) $[MoO_2(L^9)(MeOH)]$: yield (orange brown powder): 59.3 mg (22.3%). C, 51.3; H, 4.5; N, 3.0; Mo, 24.2%. Calc. for $C_{19}H_{15}MoNO_5$ (M_r = 433.30): C, 51.4; H, 4.5; N, 3.0; Mo, 22.1%. IR(KBr, cm^{-1}): $1619\nu_{(C{=}N)}$; 942 and $900\nu_{(MoO_2)}$.

Ligands: all experimental details, IR spectra, PXRD data for ligands H_2L^n (n = 1, 4, 5, 7, 8 and 9) are given in Table S1 and Fig. S1–S6 (ESI†).

General procedure for the epoxidation of olefins by aqueous TBHP

For cyclooctene and limonene. A mixture of *cis*-cyclooctene (2.00 mL, 15.4 mmol) or (*R*)-limonene (2.5 mL, 15.4 mmol), 0.1 mL acetophenone (internal reference) and Mo (pre)catalyst (0.5% catalyst loading, 0.077 mmol) was stirred and heated up to 80 °C before adding aqueous TBHP (70 wt%, 4.25 mL, 30.8 mmol).

For cyclohexene. A mixture of cyclohexene (1.6 mL, 15.8 mmol), dodecane (internal reference) and Mo (pre)catalyst (0.5% catalyst loading, 0.079 mmol) was stirred and heated up to 80 °C before adding aqueous TBHP (70 wt%, 4.38 mL, 31.6 mmol).

The catalytic experiments were performed with a 0.5/200/100 Mo/TBHP/alkene molar proportion. All the reactions were performed for 4 h. Aliquots (0.1 mL) of organic phase were taken at required times from the reaction media, mixed with 2 mL of Et_2O and a small quantity of MnO_2 was added. The mixture was then filtered through silica and analyzed by GC.

Acknowledgements

Prof. Višnja Vrdoljak is acknowledged for useful discussions during the writing of the article. This research was supported by the Ministry of Science, Education and Sports of the Republic of Croatia.

References

1 R. A. Sheldon, *Green Chem.*, 2007, **9**, 1273.

2 (*a*) C. Wang, X. Wu, S. Tu and B. Jiang, *Synth. React. Inorg., Met.-Org., Nano-Met. Chem.*, 2009, **39**, 78; (*b*) P. Panneerselvam, R. R. Nair, G. Vijayalakshmi, E. H. Subramanian and S. K. Sridhar, *Eur. J. Med. Chem.*, 2005, **40**, 225; (*c*) W. Lu, Y. H. Huang, S. I. Lo and H. H. Wei, *Inorg. Chem. Commun.*, 2007, **10**, 1210; (*d*) N. C. Gianneschi, S. T. Nguyen and C. A. Mirkin, *J. Am. Chem. Soc.*, 2005, **127**, 1644; (*e*) M. R. Maurya, A. K. Chandrakar and S. Chand, *J. Mol. Catal. A: Chem.*, 2007, **270**, 225; (*f*) M. R. Maurya, A. Arya, P. Adao and J. C. Pessoa, *Appl. Catal., A*, 2008, **351**, 239; (*g*) G. Grivani, A. D. Khalaji, V. Tahmasebi, K. Gotoh and H. Ishida, *Polyhedron*, 2012, **31**, 265; (*h*) S. Rayati, M. Koliaei, F. Ashouri, S. Mohebbi, A. Wojtczak and A. Kozakiewicz, *Appl. Catal., A*, 2008, **346**, 65.

3 (*a*) J. Kollar, *US Pat.*, 3350422, Halcon International, 1967; (*b*) J. Kollar, *US Pat.*, 3351635, Halcon International, 1967; (*c*) J. Kollar, *US Pat.*, 3507809, Halcon International, 1970; (*d*) J. Kollar, *US Pat.*, 3625981, Halcon International, 1971; (*e*) M. N. Sheng and G. J. Zajaczek, *GB 1.136.923*, 1968; (*f*) K. A. Jorgensen, *Chem. Rev.*, 1989, **89**, 431; (*g*) B. S. Lane and K. Burgess, *Chem. Rev.*, 2003, **103**, 2457; (*h*) F. E. Kühn, A. M. Santos and M. Abrantes, *Chem. Rev.*, 2016, **106**, 2455.

4 (*a*) R. Martos Calvente, J. M. Campos-Martin and J. L. G. Fierro, *Catal. Commun.*, 2002, **3**, 247; (*b*) K. Dallmann, R. Buffon and W. Loh, *J. Mol. Catal. A: Chem.*, 2002, **178**, 43.

5 (*a*) K. Nakayima, K. Yokoyama, T. Kano and M. Kojima, *Inorg. Chim. Acta*, 1998, **282**, 209; (*b*) C. P. Rao, A. Sreedhara, P. V. Rao, N. K. Lokanath, M. A. Sridhar, J. S. Prasad and K. Rissanen, *Polyhedron*, 1999, **18**, 289; (*c*) C. A. Mcauliffe, F. P. Mc Cullough, M. J. Parrott, C. A. Rice, B. J. Sayle and W. Levanson, *J. Chem. Soc., Dalton Trans.*, 1977, 1762; (*d*) E. C. Alyea and A. Malek, *Can. J. Chem.*, 1975, **53**, 939; (*e*) A. Elmali and Y. Elerman, *J. Mol. Struct.*, 1998, **442**, 31; (*f*) A. Elmali, Y. Elerman and C. T. Zeyrek, *J. Mol. Struct.*, 1998, **443**, 123; (*g*) M. Kabak, A. Elmali and Y. Elerman, *J. Mol. Struct.*, 1999, **477**, 151; (*h*) A. Elmali, M. Kabak and Y. Elerman, *J. Mol. Struct.*, 1999, **484**, 229; (*i*) V. Barba, D. Cuahutle, R. Santillan and N. Farfán, *Can. J. Chem.*, 2001, **79**, 1229; (*j*) P. G. Lacroix, F. Averseng, I. Malfant and K. Nakatani, *Inorg. Chim. Acta*, 2004, **357**, 3825; (*k*) V. T. Kasumov, S. Özal-Yaman and E. Tas, *Spectrochim. Acta, Part A*, 2005, **62**, 716; (*l*) R. Kannappan, D. M. Tooke, A. L. Spek and J. Reedijk, *Inorg. Chim. Acta*, 2006, **359**, 334; (*m*) M. Rodríguez, R. Santillan, Y. López, N. Farfán, V. Barba, K. Nakatani, E. V. García Baéz and I. I. Padilla-Martínez, *Supramol. Chem.*, 2007, **19**, 641.

6 (*a*) J. M. Brégeault, *J. Chem. Soc., Dalton Trans.*, 2003, 3289; (*b*) Z. Dawoodi and R. L. Kelly, *Polyhedron*, 1986, **5**, 271; (*c*) D. D. Agarwal and S. Shrivastava, *Polyhedron*, 1988, **7**, 2569; (*d*) D. D. Agarwal, *J. Mol. Catal.*, 1988, **44**, 65; (*e*) J. M. Sobczak and J. J. Ziolkowski, *Appl. Catal. A Chem.*, 2003, **248**, 261; (*f*) M. Bagherzadeh and S. G. Esfahani, *Sci. Iran., Trans. C*, 2010, **17**, 131; (*g*) J. Zhao, X. Zhou, A. M. Santos, E. Herdtweck, C. C. Romão and F. E. Kühn, *Dalton Trans.*, 2003, 3736; (*h*) S. L. Pandhare, R. R. Jadhao, V. G. Puranik, P. V. Joshi, F. Capet, M. K. Dongare, S. B. Umbarkar, C. Michon and F. Agbossou-Niedercorn, *J. Organomet. Chem.*, 2014, **772–773**, 271.

7 I. P. Beleteskaya and L. M. Kustov, *Russ. Chem. Rev.*, 2010, **79**, 441.

8 (*a*) J. Morlot, N. Uyttebroeck, D. Agustin and R. Poli, *ChemCatChem*, 2013, **5**, 601; (*b*) W. Wang, T. Vanderbeeken, D. Agustin and R. Poli, *Catal. Commun.*, 2015, **63**, 26; (*c*) J. Pisk, D. Agustin, J. C. Daran, V. Vrdoljak and R. Poli,

Adv. Synth. Catal., 2011, **353**, 2910; (*d*) J. Pisk, B. Prugovečki, D. Matković-Čalogović, R. Poli, D. Agustin and V. Vrdoljak, *Polyhedron*, 2012, **33**, 441; (*e*) J. Pisk, B. Prugovečki, D. Matković-Čalogović, T. Jednačak, P. Novak, D. Agustin and V. Vrdoljak, *RSC Adv.*, 2014, **4**, 39000; (*f*) V. Vrdoljak, J. Pisk, D. Agustin, P. Novak, J. Parlov Vuković and D. Matković-Čalogović, *New J. Chem.*, 2014, **38**, 6176; (*g*) C. Cordelle, D. Agustin, J. C. Daran and R. Poli, *Inorg. Chim. Acta*, 2010, **364**, 144; (*h*) B. Guérin, D. Mesquita Fernandes, J.-C. Daran, D. Agustin and R. Poli, *New J. Chem.*, 2013, **37**, 3466; (*i*) W. Wang, T. Guerrero, S. R. Merecias, H. García-Ortega, R. Santillan, J.-C. Daran, N. Farfán, D. Agustin and R. Poli, *Inorg. Chim. Acta*, 2015, **431**, 176; (*j*) J. Pisk, J.-C. Daran, R. Poli and D. Agustin, *J. Mol. Catal. A: Chem.*, 2015, **403**, 52; (*k*) W. Wang, J.-C. Daran, R. Poli and D. Agustin, *J. Mol. Catal. A: Chem.*, 2016, **416**, 117.

9 (*a*) K. Yamaguchi, K. Kamata, S. Yamaguchi, M. Kotani and N. Mizuno, *J. Catal.*, 2008, **258**, 121; (*b*) J. Kasai, Y. Nakagawa, S. Uchida, K. Yamaguchi and N. Mizuno, *Chem. – Eur. J.*, 2006, **12**, 4176.

10 (*a*) A. V. Trask, W. D. S. Motherwell and W. Jones, *Chem. Commun.*, 2004, 890; (*b*) N. Shan, F. Toda and W. Jones, *Chem. Commun.*, 2002, 2372; (*c*) D. Braga, S. L. Giaffreda, F. Grepioni, A. Pettersen, L. Maini, M. Curzi and M. Polito, *Dalton Trans.*, 2006, 1249.

11 (*a*) M. Cindrić, N. Strukan, V. Vrdoljak, T. Kajfež and B. Kamenar, *Z. Anorg. Allg. Chem.*, 2002, **628**, 2113; (*b*) D. Agustin, C. Bibal, B. Neveux, J.-C. Daran and R. Poli, *Z. Anorg. Allg. Chem.*, 2009, **635**, 2120; (*c*) M. Cindrić, N. Strukan, V. Vrdoljak and B. Kamenar, *Z. Anorg. Allg. Chem.*, 2004, **630**, 585.

12 B. Kaitner and M. Zbačnik, *Acta Chim. Slov.*, 2012, **59**, 670.

13 (*a*) O. A. Rajan and A. Chakravorty, *Inorg. Chem.*, 1981, **20**, 660; (*b*) T. Glowiak, L. Jerzykiewicz, J. M. Sobczak and J. J. Ziolkowski, *Inorg. Chim. Acta*, 2003, **356**, 387; (*c*) C. Zhang, G. Rheinwald, V. Lozan, B. Wu, P.-G. Lassahn, H. Lang and C. Janiak, *Z. Anorg. Allg. Chem.*, 2002, **628**, 1259; (*d*) P. K. Nath and K. C. Dash, *Transition Met. Chem.*, 1985, **10**, 262; (*e*) J. M. Sobczak, T. Glowiak and J. J. Ziolkowski, *Transition Met. Chem.*, 1990, **15**, 208.

14 (*a*) P. K. Nath and K. C. Dash, *Transition Met. Chem.*, 1985, **10**, 262; (*b*) J. M. Sobczak, T. Glowiak and J. J. Ziolkowski, *Transition Met. Chem.*, 1990, **15**, 2008; (*c*) W.-S. Jung, H.-Y. Moon and Y.-Y. Park, *Polyhedron*, 1997, **16**, 2169; (*d*) J. Topich, *Inorg. Chim. Acta*, 1981, **20**, 3704.

15 M. Minelli, F. Namuswe, D. Jeffrey, A. L. Morrow, I. A. Guzei, D. Swenson, E. Bothe and T. Weyhermüller, *Inorg. Chem.*, 2006, **45**, 5455.

16 G. J. J. Chen, J. W. McDonald and W. E. Newton, *Inorg. Chem.*, 1976, **15**, 2612.

17 Oxford Diffraction Ltd, Xcalibur CCD system, *CrysAlis* Software system, Versions 1.171.32.24 and 1.171.33.41. Abingdon; Oxfordshire, England, 2008.

18 G. M. Sheldrick, A short history of SHELX., *Acta Crystallogr., Sect. A: Found. Crystallogr.*, 2008, **A64**, 112.

19 L. J. Farrugia, WinGX (Ver. 1.80.05) suite for small-molecule single-crystal crystallography, *J. Appl. Crystallogr.*, 1999, **32**, 837.

20 L. Spek, A Multipurpose Crystallographic Tool, *J. Appl. Crystallogr.*, 2003, **36**, 7.

21 L. J. Farrugia, Ortep-3 for Windows (v. 2.02) – a version of the current release of ORTEP-III, which incorporates a Graphical User Interface (GUI), *J. Appl. Crystallogr.*, 1997, **30**, 565.

22 C. F. Macrae, I. J. Bruno, J. A. Chisholm, P. R. Edgington, P. McCabe, E. Pidcock, L. Rodriguez-Monge, R. Taylor, M. Towler, J. Van der Streek and P. A. Wood, *J. Appl. Crystallogr.*, 2008, **41**, 466.

23 *X'Pert Software Suite, Version 1.3e*, Panalytical B. V., Almelo, The Netherlands, 2001.